2672 *Biochemistry* **2010,** *49,* 2672–2679
DOI: 10.1021/bi901432d

BIOCHEMISTRY
including biophysical chemistry & molecular biology
Article

Succinylphosphonate Esters Are Competitive Inhibitors of MenD That Show Active-Site Discrimination between Homologous α-Ketoglutarate-Decarboxylating Enzymes[†]

Maohai Fang,[‡] R. Daniel Toogood,[‡] Andrea Macova,[‡] Karen Ho,[‡] Scott G. Franzblau,[§] Michael R. McNeil,[∥] David A. R. Sanders,[‡] and David R. J. Palmer*,[‡]

[‡]*Department of Chemistry, University of Saskatchewan, 110 Science Place, Saskatoon, SK S7N 5C9, Canada,* [§]*Institute for Tuberculosis Research, College of Pharmacy, University of Illinois, 833 South Wood Street, Chicago, Illinois 60612, and* [∥]*Department of Microbiology, Immunology and Pathology, Colorado State University, Fort Collins, Colorado 80523*

Received August 14, 2009; Revised Manuscript Received February 18, 2010

ABSTRACT: MenD is a thiamin diphosphate-dependent enzyme catalyzing the first unique step in menaquinone biosynthesis in bacteria. We have synthesized acylphosphonate ester analogues of α-ketoglutarate, a substrate of MenD. These compounds are competitive inhibitors of MenD, with K_i values as low as 700 nM. Observed structure−activity relationships are in notable contrast to those reported previously for succinylphosphonate inhibition of the α-ketoglutarate dehydrogenase complex, despite the apparent homology of these enzymes, and the identical decarboxylation reactions catalyzed. Inhibiting menaquinone biosynthesis is a proposed approach to inhibiting *Mycobacterium tuberculosis* growth. These inhibitors showed no significant inhibition of *M. tuberculosis* growth in vitro under aerobic and hypoxic conditions but give new information about the binding characteristics of the MenD active site. Site-directed mutation of Ser391 to alanine had only a minor effect on catalysis, but even the conservative mutation of Arg395 to lysine had a significant effect on the catalytic processing of isochorismate.

MenD is an enzyme required for menaquinone (vitamin K_2) biosynthesis in many bacteria (*1*, *2*). The biosynthetic pathway for menaquinone begins with the reversible conversion of chorismate to isochorismate by the gene product MenF, followed by a thiamin diphosphate-dependent decarboxylation and carboligation catalyzed by MenD. The MenD-catalyzed reaction is shown in Scheme 1.

MenD is a member of a family of homologous thiamin diphosphate-dependent decarboxylases that includes pyruvate decarboxylase, pyruvate dehydrogenase (PDH),[1] benzoylformate decarboxylase (BFDC), the α-ketoglutarate dehydrogenase complex (KGDHC), and others (*3*, *4*). MenD shares a common chemical step with these enzymes, the ThDP-dependent decarboxylation of a 2-oxo acid, in this case α-ketoglutarate (also called 2-oxoglutarate). MenD is unique, however, in that it catalyzes formation of a new carbon−carbon bond between the decarboxylated substrate and the *β*-carbon of a second substrate, isochorismate; the closest nonenzymatic equivalent is a Stetter reaction (*5*). MenD has also been called 2-succinyl-6-hydroxy-2,4-cyclohexadiene-1-carboxylate (SHCHC) synthase for many years (*6*−*8*), but Jiang et al. have shown that MenD releases 2-succinyl-5-enolpyruvyl-6-hydroxy-3-cyclohexene-1-carboxylate (SEPHCHC) (*9*), which is subsequently converted to SHCHC by another enzyme, MenH (*10*). MenD is presumed to follow a ping-pong kinetic mechanism; i.e., the ThDP-dependent decarboxylation of α-ketoglutarate occurs prior to the binding and reaction of isochorismate, as shown in Scheme 2, although experiments demonstrating the kinetic mechanism have not been published. Recently, the medium-resolution structure of the *Escherichia coli* MenD·ThDP·Mn^{2+} complex was published (*11*).

Phosphonate analogues of 2-oxo acids can act as inhibitors of ThDP-dependent decarboxylases. For example, methyl acetylphosphonate and methyl benzoylphosphonate are reversible inhibitors of PDH (*12*, *13*) and BFDC (*14*) respectively, while benzoylphosphonate is an inactivator of BFDC, phosphorylating an active-site serine residue (*15*). Bunik et al. showed that the brain α-ketoglutarate dehydrogenase complex (KGDHC) is inhibited by some derivatives of succinylphosphonate (4-phosphono-4-oxobutanoate, **1**) (*16*). These authors found **1** and its monoethyl phosphonate ester to be reversible inhibitors of KGDHC. In contrast, acetylphosphonate shows little or no inhibition of PDH, suggesting the second negative charge is deleterious to inhibition for this enzyme. Benzoylphosphonate inactivation of BFDC indicates that this dianionic inhibitor binds to the active site. Thus, despite a similar chemical reaction catalyzed in a conserved ThDP-binding site, the behavior of acylphosphonates cannot be predicted with certainty.

Scheme 1

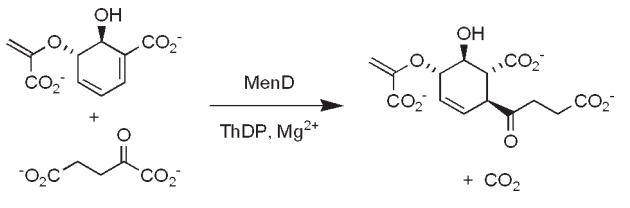

[†]This work was supported by an NSERC Discovery Grant to D.R.J.P. and a Saskatchewan Health Research Fund Team Grant to the Molecular Design Research Group.

*To whom correspondence should be addressed. Telephone: (306) 966-4662. Fax: (306) 966-4730. E-mail: dave.palmer@usask.ca.

[1]Abbreviations: BFDC, benzoylformate decarboxylase; KGDHC, brain α-ketoglutarate dehydrogenase complex; KGDC E1, *E. coli* α-ketoglutarate dehydrogenase E1 subunit; PDH, pyruvate dehydrogenase; SHCHC, 2-succinyl-6-hydroxy-2,4-cyclohexadiene-1-carboxylate; SEPHCHC, 2-succinyl-5-enolpyruvyl-6-hydroxy-3-cyclohexene-1-carboxylate; ThDP, thiamine diphosphate.

 Published on Web 03/03/2010

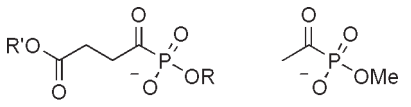

1: R = H, R' =H
2: R = Me, R' = H
3: R = Et, R' = H
4: R = Pr^i, R' = H
5: R = Me, R' = Me
6: R = Me, R' = Et
7: R = Me, R' = Bn
8: R = Et, R' = Bn
9: R = Pr^i, R' = Bn

10

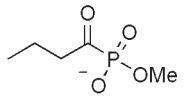

11

MenD and KGDHC catalyze the identical decarboxylation reaction, although there is considerable variation of the two active sites, with the exception of a small group of residues that interact directly with the cofactors (*11*, *17*). As described above, substrate analogues of α-ketoglutarate were synthesized to inhibit KGDHC, based on the chemical reaction, i.e., without explicit consideration of the active-site structure. These inhibitors would be predicted to inhibit MenD also, but the differences in the active-site topology may result in different structure−activity relationships.

Inhibition of MenD may be of considerable interest because many bacteria, including *Mycobacterium tuberculosis*, rely on menaquinone (vitamin K_2) as an electron acceptor, allowing respiration under low-oxygen conditions (*1*, *2*). Tuberculosis infections can therefore persist under hypoxic conditions for long periods of time (*18*). Controlling the intracellular concentration of menaquinone can inhibit the growth of *M. tuberculosis* (*19*, *20*), and the menaquinone biosynthetic pathway has been proposed as a target for antibiotic, especially antituberculosis, drugs (*21*, *22*). If MenD is to serve as a target for antibiotics, then inhibitor selectivity will be a primary concern.

We have therefore explored the ability of succinylphosphonate derivatives to inhibit MenD. We hypothesized that an α-ketoglutarate mimic such as methyl succinylphosphonate (**2**) would bind to the active site and react with ThDP to give a dead-end complex, as observed for PDH and BFDC, but we could not rule out the possibility that **1** would act as an inhibitor, as seen with KGDHC. Ideally, inhibitors distinct from those that inhibit mammalian enzymes would be lead compounds for antibacterial drug design. To test our hypotheses, we synthesized 11 acylphosphonates, including four novel compounds, and measured their inhibitory properties with respect to MenD, and their antibiotic properties. Site-directed mutagenesis was then used to probe the roles of two key residues from the active site of MenD.

Scheme 2

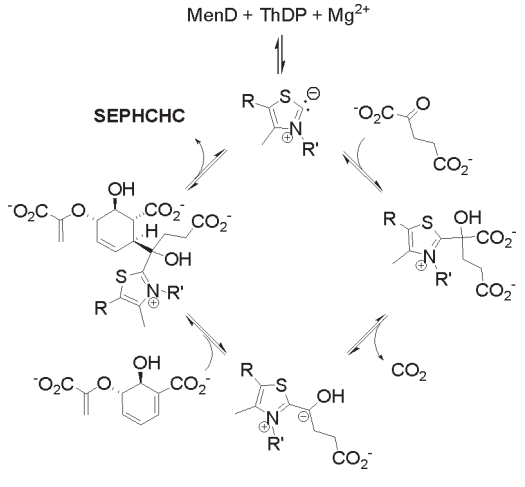

MATERIALS AND METHODS

Synthesis of Inhibitors. (*i*) *General*. Experiments that required anhydrous conditions were performed under an inert atmosphere of either dry argon or nitrogen gas. Glassware was dried overnight in an oven set at 120 °C and assembled under a stream of inert gas. All reagents were obtained from commercial suppliers and unless indicated otherwise used without further purification. Dichloromethane was freshly distilled from calcium hydride. Thin layer chromatography (TLC) was performed on precoated silica gel plates (Merck Kieselgel $60F_{254}$, 0.25 mm thickness) and visualized with phosphomolybdic acid reagent, iodine vapors, or ultraviolet light at 254 nm. Flash chromatography was performed using Merck silica gel 60 (230−400 mesh). NMR spectra were recorded using a Bruker 500 MHz spectrometer with samples dissolved in the appropriate deuterated solvents. Chemical shifts were reported in parts per million downfield from tetramethylsilane. Mass spectrometry was performed on an API Qstar XL pulsar hybrid lc/ms/ms apparatus. Melting points were measured on a Gallencamp melting point apparatus and were not corrected. NMR, mass spectrometry, and elemental analysis facilities were a part of the Saskatchewan Structural Sciences Centre. Chemical reagents, including buffers, salts, and fine chemicals, were obtained from Sigma-Aldrich Canada, Ltd. (Oakville, ON) or VWR CanLab (Mississaugua, ON) and were categorized as molecular biology grade or were the highest grade available.

(*ii*) *General Procedure for the Preparation of Succinylphosphonates*. Succinic anhydride was treated with the appropriate alcohol to form the corresponding monoester (*23*, *24*). The succinate monoester was converted to the acid chloride at 0 °C, using 1.1 equiv of oxalyl chloride dissolved in CH_2Cl_2 containing one drop of DMF. The acid chloride was reacted at 0 °C with 1 equiv of the appropriate trialkyl phosphite. Succinylphosphonates **1**−**4** were made from the monobenzyl ester, and the benzyl group was subsequently removed by hydrogenolysis over 10% Pd/C in a solution of EtOAc and formic acid at atmospheric pressure (using a H_2-filled balloon). Alkyl phosphonate esters were cleaved using stoichiometric amounts of LiBr or NaI in acetonitrile. Details and characterization are supplied in the Supporting Information.

Enzymology. (*i*) *General*. Cultures were grown in an Innova 4230 incubator shaker and were lysed using a Virsonic 600 ultrasonic cell disrupter. A BioCAD Sprint Perfusion Chromatography system was routinely used for large-scale protein purifications and the Bio-Rad Mini-protean 3 used to assess protein purity. Chelating Sepharose FF columns were purchased from GE Healthcare (Baie D'Urfe, QC). Centrifugation was performed using either a Beckman Coulter microfuge 18 and 22R centrifuge or a Beckman J2-HS refrigerated centrifuge with a JLA-10.5 or JA-25.5 rotor.

(*ii*) *Protein Purification*. The *menD* gene was subcloned into the BamHI and KpnI sites of vector pQE80-L (QIAgen, Mississauga, ON) by PCR amplification of the gene using oligonucleotide primers incorporating these restriction sites, followed by standard ligation procedures and transformation of *E. coli* Nova Blue (Novagen, VWR-Canlab). The insert of the resulting plasmid was sequenced (National Research Council Plant

Biotechnology Institute DNA Technologies Unit, Saskatoon, SK) to ensure no mutations had been introduced.

Gene expression was induced in a Nova Blue cell culture, shaken at 225 rpm and 37 °C in LB broth containing 50 mg/L ampicillin, by induction with 1 mM IPTG after the culture had reached an optical density (OD_{600}) of 0.4, followed by continued growth for 4 h at 30 °C. Cells were lysed by sonication in buffer containing 5 mM imidazole, 0.5 M sodium chloride, 12.5% glycerol, and 20 mM Tris-HCl (pH 7.9). The protein was purified by being bound to a Ni^{2+}-charged NTA column, washed with the same buffer containing 50 mM imidazole, and then eluted with buffer containing 50 mM EDTA. The purified protein was dialyzed into 5 mM Tris-HCl (pH 7.4) and 50% glycerol. Protein was stored in 0.4 mL aliquots at −80 °C after being snap-frozen in liquid nitrogen.

(*iii*) *Wild-Type Enzyme Assays*. Isochorismate was prepared as described previously (*8*). The isochorismate concentration was determined enzymatically, by measuring the drop in absorbance at 278 nm in the presence of MenD and excess α-ketoglutarate, using an extinction coefficient ε of 8300 M^{-1} cm^{-1} (*25*). Isochorismate consistently accounted for ~80% of the absorbance at 278 nm. All assays were conducted at 25 °C using a Beckman Coulter DU 640 spectrophotometer and were performed in a total volume of 1 mL with a final concentration of 100 mM Tris-HCl (pH 7.4). Apparent rate constants for isochorismate, α-ketoglutarate, ThDP, and $MgCl_2$ were determined via variation of each substrate or cofactor in saturating concentrations of the others, namely, 5 mM $MgCl_2$, 50 μM ThDP, 100 μM α-ketoglutarate, and 20 μM isochorismate. The MenD concentration was 10 nM. The isochorismate solution was freshly prepared before each experiment.

The reaction rate was measured by continuously monitoring the absorbance change at 278 nm due to the disappearance of isochorismate. All rates measured were corrected with a blank reaction in the absence of isochorismate. All data points represent the average of at least two experiments. Kinetic constants were determined using Leonora (*26*) by nonlinear least-squares fitting of the data to the Michaelis−Menten equation (eq 1)

$$v = V_{max}[S]/(K_m + [S]) \quad (1)$$

where v is the measured rate, V_{max} is the apparent maximal rate, K_m is the apparent Michaelis constant, and [S] is the concentration of the varied substrate. The apparent turnover number, k_{cat}, is calculated from V_{max} by dividing by the enzyme concentration.

(*iv*) *Inhibition Study of* α*-Ketoglutarate Phosphonate Analogues*. The reaction mixture contained all components and appropriate inhibitors but α-ketoglutarate. MenD at a final concentration of 60 nM was used, and the isochorismate concentration was fixed at 20 μM for the assay. After preincubation at 25 °C for 3 min, the reaction was initiated by addition of α-ketoglutarate with various concentrations (10, 15, 20, and 40 μM) at five fixed concentrations of each inhibitor. The inhibition type and the inhibition constants were determined graphically with a Dixon plot (*27*) ($1/v$ vs inhibitor concentration at four different α-ketoglutarate concentrations) and a Cornish-Bowden plot (*28*) (α-ketoglutarate concentration/v vs inhibitor concentration at four different α-ketoglutarate concentrations), based on eq 2

$$v = \frac{V_{max}[S]}{[S] + K_m\left(1 + \frac{[I]}{K_i}\right)} \quad (2)$$

where [I] is the inhibitor concentration, K_i is the inhibition constant, and [S] is the concentration of the substrate α-ketoglutarate.

Reversibility of inhibition was tested by dilution. MenD was incubated for 3 min in 10 mM **2** and then diluted 150-fold under normal assay buffer conditions. The MenD-catalyzed reaction rate resulting from this treatment was identical to the blank.

To test for the time dependence of inhibition, all reagents, including 100 μM α-ketoglutarate, 20 μM isochorismate, and 100 or 400 μM **2**, were equilibrated at 25 °C, before initiation of the reaction via addition of MenD (final concentration of 60 nM). The resulting progress curve was linear, with no lag or apparent increase in the level of inhibition over 30 min. The same was observed when the reaction was instead initiated by addition of isochorismate.

(*v*) *Site-Directed Mutagenesis*. Point mutations were generated using the QuikChange site-directed mutagenesis kit from Stratagene (La Jolla, CA) according to the manufacturer's directions, except that an extension time of 2 min per kilobase gave better results than the recommended time of 1 min per kilobase. For each mutant, a mutagenic primer was designed to incorporate a change in the nucleotide sequence encoding the residue of interest. For other mutants, an additional, silent mutation was introduced to generate a new restriction site for the purpose of screening, after transformation of *E. coli* XL1-Blue with PCR-amplified DNA. A complete list of primer sequences is included in the Supporting Information.

After transformants had been screened, selected clones were tested for expression by transformation of *E. coli* BL-21Gold. All selected clones exhibited expression similar to that of the wild-type enzyme. A clone was selected, and the complete gene was sequenced (National Research Council Plant Biotechnology Institute DNA Technologies Unit) to ensure no other mutations had been introduced. The protein was purified as previously described for the wild-type enzyme, but using columns which had never been in contact with wild-type MenD.

Susceptibility Studies. *M. tuberculosis* H37Rv grown to midlog in 7H9-OADC medium containing 0.05% Tween 80 was diluted to 2×10^5 colony forming units/mL for use in these assays. Each well in a 96-well round-bottomed microtiter plate received 4 μL of compound in DMSO at its respective concentration, 96 μL of 7H9-OADC Tween 80 medium, and 100 μL of the diluted H37Rv cells. The starting concentration for each compound was 200 μg/mL (4 μL of compound in DMSO at 10 mg/mL in a total volume of 200 μL) and serially titrated down 2-fold to as low as 0.4 μg/mL (final concentration). The plates were incubated for 10 days at 37 °C and scanned for visual density reads. Wells with no visible settling of cells (clear well) were considered null, and any settling seen was considered positive. MIC_{100} is the first completely clear well.

The low-oxygen recovery assay (LORA) and microplate Alamar Blue assay (MABA) were performed following published procedures (*29*, *30*).

RESULTS AND DISCUSSION

Measuring Rate Constants with MenD. Jiang et al. effectively showed that monitoring the disappearance of isochorismate (by UV spectroscopy at 278 nm) is the only reliable way to measure the rate of the MenD-catalyzed reaction, since the product (SEPHCHC) is essentially UV-silent (*9*). Although isochorismate is prone to spontaneous decomposition (*31*), careful handling of this compound and storage at −80 °C gives

Table 1: Kinetic Constants Determined for MenD and Its Mutants

enzyme	K_m(α-ketoglutarate) (μM)	K_m(ThDP) (μM)	K_m(Mg^{2+}) (μM)	K_m(isochorismate) (μM)	k_{cat} (min^{-1})
wild type	9.9 ± 0.6	8 ± 1	44 ± 1	ND[a]	17 ± 3
S391A	13 ± 1	17 ± 1	13 ± 1	ND	18 ± 1
S391Y			trace activity		
R395K	45 ± 3	2.2 ± 0.2	ND	5.3 ± 0.9	8.7 ± 0.5
R395A	ND[b]	ND	ND	36[c]	2.5[c]

[a]ND, not determined. The apparent K_m for isochorismate is below the limit of accurate measurement (see the text). [b]The apparent K_m values for α-ketoglutarate and cofactors could not be determined because of the high UV absorbance resulting from concentrations of isochorismate necessary for saturation. [c]Value estimated from the Hanes−Woolf plot.

consistent results, but the isochorismate concentration must be determined enzymatically before kinetic experiments are performed. HPLC analysis of a MenD reaction mixture shows that in the presence of excess α-ketoglutarate, all isochorismate is consumed (data not shown).

An inherent challenge is presented by the very low K_m value exhibited by isochorismate. The K_m value was previously measured (*9*) to be well below 1 μM, and we concur with this finding. However, this precludes accurate rate measurements at isochorismate concentrations below K_m, since even a 100 nM solution, approximately twice the K_m estimated previously, has an absorbance of only 0.00083 AU. Thus, an accurate apparent K_m value for isochorismate cannot be measured. This also makes experiments in which both substrates are varied, such as those that would normally be used to diagnose a ping-pong mechanism, impossible, since values near the Michaelis constant are appropriate for these experiments. Apparent values for α-ketoglutarate, as well as cofactors ThDP and Mg^{2+}, can be measured in a straightforward manner by saturation with isochorismate.

MenD was expressed from a plasmid derived from pQE80-L, resulting in a homogeneous protein bearing an N-terminal hexahistidine tag. Kinetic constants, listed in Table 1, differ slightly from those determined by Jiang et al. (*9*). These authors reported a lower apparent k_{cat} (4.5 min^{-1}) and K_m (1.5 μM) for α-ketoglutarate, a lower K_m for ThDP (2.4 μM), and a higher K_m for Mg^{2+} (80 μM). Some of the variation may be attributable to differences in reaction temperatures and conditions.

Synthesis of Inhibitors. Acylphosphonates were synthesized on the basis of the Arbuzov reaction as described by Karaman et al. (*32*). Formation of a succinate monoester, followed by conversion of the acid to the acid chloride, allowed formation of the carbon−phosphorus bond using a trialkyl phosphite as a nucleophile. The resulting phosphonate esters were typically cleaved using a stoichiometric quantity of LiBr. This approach allowed preparation of succinylphosphonate (**1**) in >70% yield and methyl succinylphosphonate (**2**) in >60% yield starting from succinic anhydride. Carboxylic esters (see below), requiring one fewer synthetic step, were isolated in higher yields. This is an improvement on other reported methods for preparing such compounds; in particular, harsh conditions were avoided by making use of the benzyl ester protecting group. Bunik's reported method (*16*) for the hydrolysis of phosphonate esters with aqueous sodium hydroxide did not give satisfactory results in our hands. Our approach is versatile in that an array of acylphosphonates could be prepared in this manner.

MenD Inhibition. The first question to be addressed was whether succinylphosphonate (**1**), which is a close steric analogue of α-ketoglutarate, or methyl succinylphosphonate (**2**), which is more similar in charge to the substrate, would act as an inhibitor. Analogy with KGDHC predicts **1** and **2** would be competitive

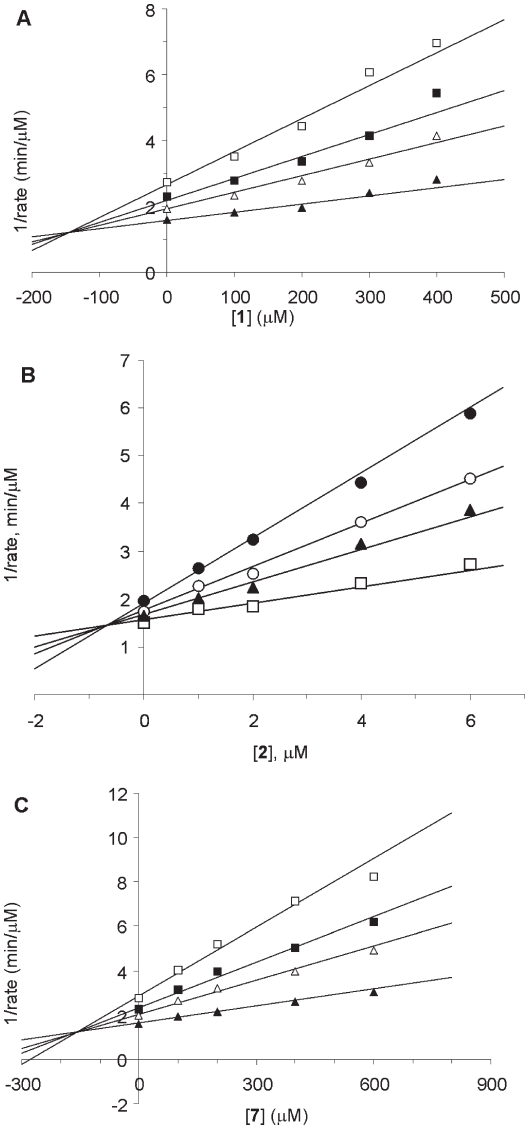

FIGURE 1: Representative Dixon plots showing competitive inhibition. Points indicate the average of at least two experiments, and the lines represent a nonlinear least-squares fit to eq 2 (see Materials and Methods). The value of K_i is the *x*-intercept of the intersection of the lines; the values are given in Table 2: (A) inhibition by **1**, (B) inhibition by **2**, and (C) inhibition by **7**. Conditions are described in Materials and Methods.

inhibitors, but analogy with PDH suggests that only **2** would inhibit MenD (vide supra). The inhibitors were analyzed with a Dixon plot, as shown in Figure 1, and with a Cornish-Bowden plot (not shown). The analysis is consistent with reversible, competitive inhibition with respect to α-ketoglutarate. No evidence of time dependence was observed, consistent with previous

Table 2: Inhibition of MenD by Acylphosphonates **1**−**11**

	Inhibitor	K_i / μM
1	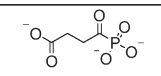	150 ± 10
2	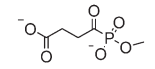	0.7 ± 0.1
3	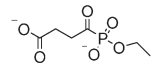	16 ± 1
4	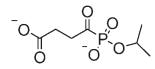	170 ± 10
5	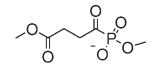	240 ± 20
6	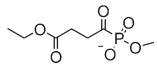	1630 ± 90
7	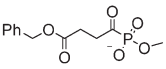	160 ± 10
8	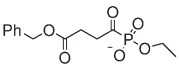	1320 ± 60
9	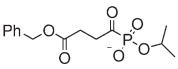	6700 ± 400
10	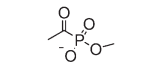	no inhibition
11	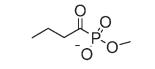	no inhibition

observations with related enzymes; for example, Bunik et al. reported no time dependence of the inhibition of KGDHC by similar compounds (*16*), and Brandt et al. reported no time dependence of the inhibition of BFDC by methyl benzoylphosphonate (*14*). It was apparent that **2** was a much better inhibitor, as shown in Table 2. Because **1** is synthesized from a methyl phosphonate precursor, inhibition observed in the presence of **1** may actually be due to a very small amount of residual **2**, since 0.5% contamination would yield the observed inhibition. A similar phenomenon was observed by Kluger and Pike in their inhibition study of PDH (*12*). This result demonstrates that although MenD and KGDHC have evolved to stabilize a transition state for the formation of an identical intermediate, the differences in active-site structure allow selective inhibition: **1** inhibits only KDGHC.

On the basis of the preference of the MenD active site for **2** over **1**, we studied other acylphosphonate monoesters. Increasing the size of the alkyl group of the phosphonate ester from methyl to ethyl (**3**) resulted in a 1 order of magnitude increase in the inhibition constant, and a further increase to isopropyl (**4**) resulted in a similar increase (Table 2).

Esterification of the carboxylate was predicted to have a detrimental effect on inhibition. Indeed, introduction of a methyl group renders the diester **5** more than 300 times less effective than **2**, while the presence of an ethyl group yields an inhibitor **6** that is 2000 times weaker than **2**. Unexpectedly, benzyl ester **7** is an improved inhibitor relative to **5** and **6**. This may be rationalized by a specific interaction of the phenyl group with the protein, such as π-stacking or cation−π stabilization; the MenD structure shows many arginine and lysine residues in the active site. The increased energy of the more hydrophobic substrate in bulk aqueous solution may also contribute to the lowered K_i value. The trend with an increase in the size of the phosphonic ester alkyl group in the presence of the benzyl ester (compounds **8** and **9**) is similar to that seen for carboxylates **2**−**4**: increasing the size sharply increases the inhibition constant. Note that Bunik et al. reported a succinylphosphonate bearing a carboxylate ester but not a phosphonate ester was an effective inhibitor, but a succinylphosphonate bearing both types of ester was not (*16*).

Although removal of the negative charge from the "carboxylate end" of these inhibitors does not remove the ability to inhibit the MenD reaction, removal of the carboxyl group itself is catastrophic to activity. Neither methyl acetylphosphonate (**10**) nor methyl butyrylphosphonate (**11**) exhibited any significant inhibition at concentrations up to 10 mM.

Antimicrobial Testing with Acylphosphonates. These compounds are the first reported inhibitors of MenD. MenD is a proposed drug target, particularly for antituberculosis drugs; therefore, we pursued the testing of these compounds as inhibitors of mycobacterial growth, under aerobic conditions and under hypoxic conditions.

Selectivity was our primary concern with respect to the use of acylphosphonates as drug candidates, given the similarity to KGDHC inhibitors, and the possibility that constitutive carboxyesterases might produce more potent phosphonate monoesters of succinylphosphonate in vivo. Bunik et al. did report that succinylphosphonate and related esters showed no significant inhibition of α-ketoglutarate-utilizing aminotransferases and dehydrogenases (*11*). Compounds were tested for their effects on the growth of *M. tuberculosis*. Unfortunately, MICs for all compounds exceeded 128 μM. Mycobacterial cell walls are well-known to be highly resistant to permeation, particularly by hydrophilic compounds (*33*).

Comparing the Active Sites of MenD and KGDHC. There is no crystal structure available for human KGDHC, but the *E. coli* α-ketoglutarate dehydrogenase E1 subunit (KDHC E1) has been crystallized and deposited in the Protein Data Bank (PDB) as entry 2JGD (*17*). The human and *E. coli* proteins are reasonably well-conserved: 38% identical and 56% similar amino acids. Therefore, comparison of *E. coli* KGDH E1 and MenD can be used to rationalize differences in inhibitor recognition. Unfortunately, no substrate is present in the KGDH E1 structure, although density identified as oxaloacetate is present, and some active-site loops are disordered. Similarly, there is no substrate or substrate analogue in the active site of the MenD crystal structure (*11*).

Despite the absence of electron density for some loops in the active site, Frank et al. (*17*) were able to identify residues in KGDH E1 that were essential to efficient catalytic activity, including His260, which was proposed to interact with a carboxylate group of α-ketoglutarate. His260 is in a well-conserved portion of the protein, as indicated in Figure 2.

MenD and KGDH E1 are distant homologues, with a low overall level of sequence identity. However, the C-terminal domain of MenD, sometimes called the PP domain because of the proximity of residues to the diphosphate region of bound ThDP, can be structurally aligned with a corresponding domain of KGDH E1. The alignment of residues 370−540 of MenD with residues 231−458 of KGDH E1 using DaliLite (*34*) is shown in

```
HUMAN  283   CEVLIPALKTIIDKSSENGVDYVIMGMPHRGRLNVLANVIRKELEQIFCQFDSKLEAADE  342
              + LIP LK +I  +  +G   V++GM HRGRLNVL NV+ K+ + +F +F  K
ECOLI  232   GDALIPMLKEMIRHAGNSGTREVVLGMAHRGRLNVLVNVLGKKPQDLFDEFAGK-HKEHL  290
```

FIGURE 2: Portion of the sequence alignment of the *Homo sapiens* KGDHC E1 component (HUMAN) and *E. coli* KGDHC E1. Residues His260 and Arg263, which align structurally with MenD residues Ser391 and Arg395, respectively, are highlighted in bold.

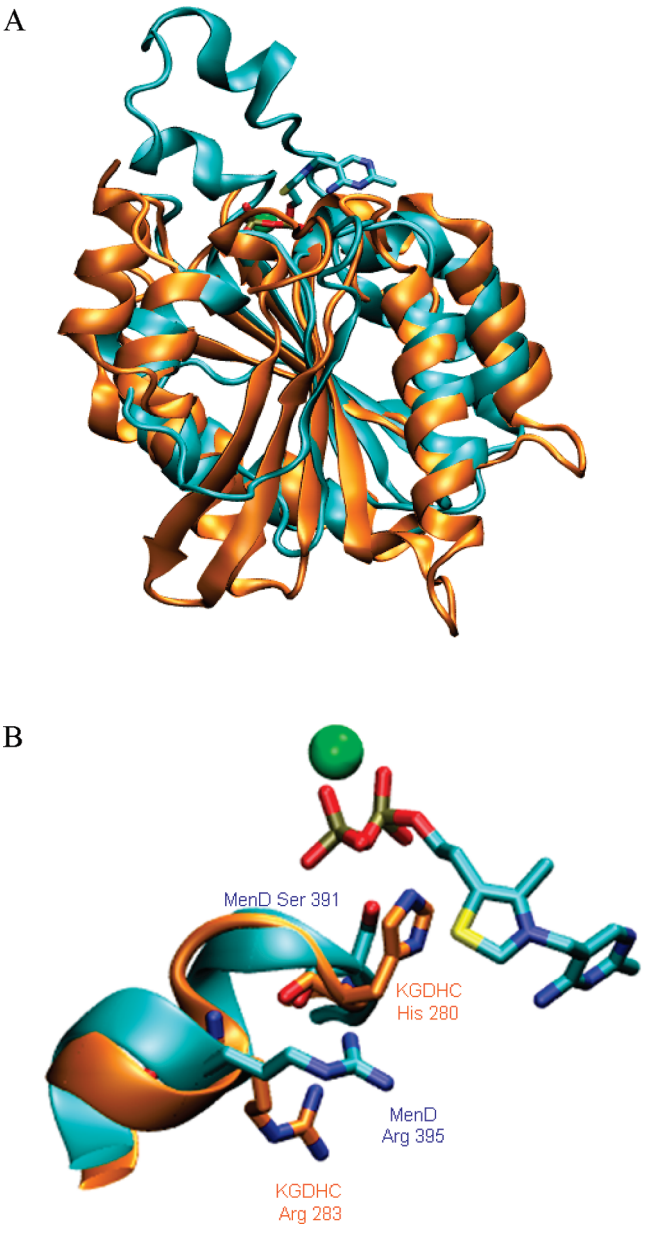

FIGURE 3: (A) Ribbon diagram of the structural alignment of residues 370−540 of MenD (cyan) with residues 231−458 of KGDH E1 (orange) using DaliLite (*34*), showing the similarity of the fold. Structural coordinates are from PDB entries 2JLA and 2JGD, respectively. ThDP and Mn^{2+} bound to MenD are included. (B) From the same alignment, showing the coincidence of MenD Ser391 and Arg395 (cyan) and KGDH E1 His280 and Arg283 (orange). Images were generated using VMD, followed by POV-Ray 3.6.

Figure 3A. This alignment results in 2.6 Å root-mean-square deviation, with 144 aligned residues, even though the level of sequence identity in this region is only 13%. As shown in Figure 3B, His260 aligns with Ser391 of MenD.

We previously predicted (*8*) that Ser391 and the nearby Arg395, which are well-conserved among MenD sequences, would likely be found at the active site of MenD and be important for catalysis. The coincidence of Ser391 with a residue known to be important in KGDH E1 catalysis suggested that this difference at the active site may contribute to differences in the recognition of phosphonate inhibitors. Figure 3B shows not only that KGDH E1 His260 and MenD Ser391 are overlapping but also that the α-carbon of MenD Arg395 aligns closely with that of KGDH E1 Arg263. The side chains of the arginine residues are in different orientations in the two structures, which may or may not be relevant given the absence of substrate from the structures. The structure of MenD shows the β-alcohol oxygen of Ser391 to be ~2.8 Å from the sulfur atom of ThDP and approximately the same distance from an oxygen atom bonded to the β-phosphorus atom (*11*). This seems to contrast with the proposed role of the structural homologue His280 in KGDHC; for these reasons, the specific role of Ser391 is ambiguous and begs investigation. Arg395, ~6.4 Å from C2 of the ThDP, seems more likely to be involved directly in interactions with isochorismate, rather than α-ketoglutarate or ThDP. However, the presence of a structural homologue in KGDH E1 argued against this role, since that enzyme does not bind isochorismate. We generated point mutants of Ser391 and Arg395 to probe their roles in catalysis.

Replacement of Ser391 with an alanine residue had surprisingly little effect on catalysis, as shown in Table 1. The turnover number is unchanged, and all parameters are within 1 order of magnitude of those of the wild-type enzyme. The most significant effect was the decrease in the apparent K_m of Mg^{2+}, followed by the increased K_m of ThDP. The lack of a large effect on catalysis suggests that Ser391 plays a structural role, or that the role is primarily served by the backbone, rather than the side chain, despite the proximity of the Ser391 alcohol group to ThDP (*11*). Alternatively, it has been proposed previously that a water molecule could bind to such a mutant so that the function of the hydroxyl group was retained, "rescuing" activity (*35*). Nonconservative mutant S391Y displayed only trace activity.

Conservative substitution of Arg395 with lysine resulted in a sharp increase in the K_m of isochorismate, to a measurable value of 5.3 μM, strongly supporting our hypothesis regarding its role in catalysis. Surprisingly, however, this mutant shows an extremely low apparent Michaelis constant with respect to Mg^{2+}. Dialyzed enzyme retains virtually all of its Mg^{2+}-dependent activity without addition of exogenous metal ion. This activity can be abolished in the presence of EDTA. This result is very difficult to rationalize; perhaps crystallization of this mutant will give some indication of why R395K seems to bind Mg^{2+} so tightly. The nonconservative substitution of Arg395 with alanine results in a mutant with significant activity, but with an even larger Michaelis constant for isochorismate. This increased value results in the inverse problem usually encountered with this enzyme: saturating values of isochorismate have an absorbance beyond the limit of the spectrophotometer, therefore, the apparent K_m values of α-ketoglutarate, ThDP, and Mg^{2+} could not be measured, and the apparent Michaelis constant of isochorismate could only be estimated to be ~36 μM using a Hanes−Woolf plot, as shown in Figure 4.

In conclusion, we have reported the first inhibitors of MenD. They are competitive with α-ketoglutarate and clearly show a

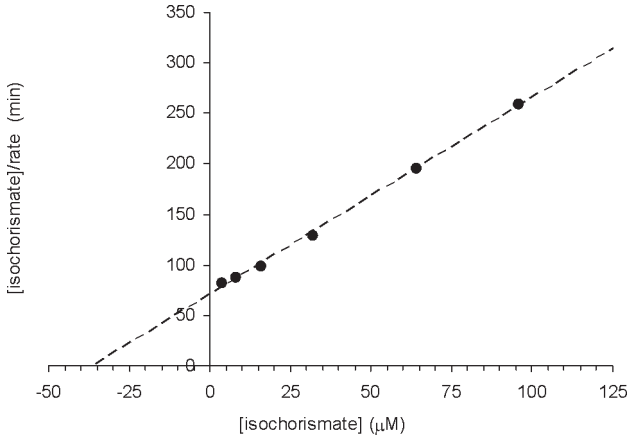

FIGURE 4: Hanes−Woolf plot used to estimate the apparent kinetic constants with respect to isochorismate in the presence of saturating concentrations of α-ketoglutarate and cofactors (see the text). Points indicate the average of at least two experiments, and the line represents the fit to the Hanes−Woolf equation (see Materials and Methods). The slope of the line gives the negative reciprocal of the apparent V_{max}; the x-intercept gives the apparent K_m. The values are listed in Table 1.

selectivity for the acylphosphonate monoester, as observed previously for BFDC, rather than the acylphosphonate, as observed for KGDHC. Inhibition most likely arises from MenD-catalyzed formation of a covalent adduct with ThDP in the active site of the enzyme. The structure−activity study indicates that a negative charge is preferred but not required in the position mimicking the δ-carboxylate of α-ketoglutarate, but the simple four-carbon analogue **11** is insufficient. A benzyl ester in this position is more potent than smaller alkyl esters. This reveals binding properties of the active site that were previously unknown. The active sites of MenD and KGDH, although apparently products of divergent evolution, both catalyze the decarboxylation of α-ketoglutarate, but mechanism-based inhibitors exhibit different structure−activity relationships.

Although some of the inhibitors, particularly **2**, are very potent, they do not exhibit antituberculosis activity in vitro. Even those bearing benzyl esters may be too polar to cross the mycobacterial cell wall. These compounds should be of use in crystallographic studies of MenD, since existing structural data do not include substrates.

Mutagenesis experiments have provided insight into the roles of two active-site residues. Ser391 can be replaced with alanine with very little effect on catalysis, showing only weak influences on the Michaelis constants of the cofactors, despite the proximity of the hydroxyl group to the thiazolium and the diphosphate moieties of ThDP. Arg395 likely interacts directly with the substrate isochorismate; this is the first experimental evidence supporting direct interaction of an amino acid of MenD with this substrate. The result is consistent with the prediction of Dawson et al. based on modeling of the medium-resolution X-ray structure of MenD (*11*).

ACKNOWLEDGMENT

We thank the Saskatchewan Health Research Foundation for funding the Molecular Design Research Group of the University of Saskatchewan, Ken Thoms and Jason Maley (Saskatchewan Structural Sciences Centre), and Kimberly Hanson.

SUPPORTING INFORMATION AVAILABLE

Preparative procedures and spectroscopic data of synthesized compounds, sequences of mutagenic primers, and an example time course of a MenD-catalyzed reaction in the absence and presence of inhibitor. This material is available free of charge via the Internet at http://pubs.acs.org.

REFERENCES

1. Meganathan, R. (1996) Biosynthesis of the isoprenoid quinones menaquinone (vitamin K2) and ubiquinone (coenzyme Q). in Escherichia coli and Salmonella: Cellular and molecular biology (Neidhart, F. C., Curtiss, R., III, Ingraham, J. L., Lin, E. C. C., Low, K. B., Magasanik, B., Reznikoff, W. S., Riley, M., Schaechter, M., and Umbarger, H. E., Eds.) pp 642−656, American Society for Microbiology, Washington, DC.
2. Meganathan, R. (2001) Biosynthesis of menaquinone (vitamin K-2) and ubiquinone (coenzyme Q): A perspective on enzymatic mechanisms. *Vitam. Horm.* (*San Diego, CA, U.S.*) *61*, 173–218.
3. Jordan, F. (2003) Current mechanistic understanding of thiamin diphosphatedependent enzymatic reactions. *Nat. Prod. Rep. 20*, 184–201.
4. Duggleby, R. G. (2006) Domain relationships in thiamine diphosphate-dependent enzymes. *Acc. Chem. Res. 39*, 550–557.
5. Myers, M. C., Bharadwaj, A. R., Milgram, B. C., and Scheidt, K. A. (2005) Catalytic conjugate additions of carbonyl anions under neutral aqueous conditions. *J. Am. Chem. Soc. 127*, 14675–14680.
6. Palaniappan, C., Sharma, V., Hudspeth, M. E. S., and Meganathan, R. (1992) Menaquinone (vitamin-K2) biosynthesis: Evidence that the *Escherichia coli* MenD gene encodes both 2-succinyl-6-hydroxy-2,4-cyclohexadiene-1-carboxylic acid synthase and α-ketoglutarate decarboxylase activities. *J. Bacteriol. 174*, 8111–8118.
7. Palaniappan, C., Taber, H., and Meganathan, R. (1994) Biosynthesis of o-succinylbenzoic acid in *Bacillus subtilis*: Identification of MenD mutants and evidence against the involvement of the α-ketoglutarate dehydrogenase complex. *J. Bacteriol. 176*, 2648–2653.
8. Bhasin, M., Billinsky, J. L., and Palmer, D. R. J. (2003) Steady-state kinetics and molecular evolution of *Escherichia coli* MenD [(1*R*,6*R*)-2-succinyl-6-hydroxy-2,4-cyclohexadiene-1-carboxylate synthase], an anomalous thiamin diphosphate-dependent decarboxylase-carboligase. *Biochemistry 42*, 13496–13504.
9. Jiang, M., Cao, Y., Guo, Z. F., Chen, M. J., Chen, X. L., and Guo, Z. H. (2007) Menaquinone biosynthesis in *Escherichia coli*: Identification of 2-succinyl-5-enolpyruvyl-6-hydroxy-3-cyclohexene-l-carboxylate as a novel intermediate and re-evaluation of MenD activity. *Biochemistry 46*, 10979–10989.
10. Jiang, M., Chen, X. L., Guo, Z. F., Cao, Y., Chen, M. J., and Guo, Z. H. (2008) Identification and characterization of (1R,6R)-2-succinyl-6-hydroxy-2,4-cyclohexadiene-1-carboxylate synthase in the menaquinone biosynthesis of *Escherichia coli*. *Biochemistry 47*, 3426–3434.
11. Dawson, A., Fyfe, P. K., and Hunter, W. N. (2008) Specificity and reactivity in menaquinone biosynthesis: The structure of *Escherichia coli* MenD (2-succinyl-5-enolpyruvyl-6-hydroxy-3-cyclohexadiene-1-carboxylate synthase). *J. Mol. Biol. 384*, 1353–1368.
12. Kluger, R., and Pike, D. C. (1977) Active-site generated analogs of reactive intermediates in enzymic reactions: Potent inhibition of pyruvate dehydrogenase by a phosphonate analog of pyruvate. *J. Am. Chem. Soc. 99*, 4504–4506.
13. Jordan, F., Nemeria, N. S., Zhang, S., Yan, Y., Arjunan, P., and Furey, W. (2003) Dual catalytic apparatus of the thiamin diphosphate coenzyme: Acid-base via the 1′,4′-iminopyrimidine tautomer along with its electrophilic role. *J. Am. Chem. Soc. 125*, 12732–12738.
14. Brandt, G. S., Kneen, M. M., Chakraborty, S., Baykal, A. T., Nemeria, N., Yep, A., Ruby, D. I., Petsko, G. A., Kenyon, G. L., McLeish, M. J., Jordan, F., and Ringe, D. (2009) Snapshot of a reaction intermediate: Analysis of benzoylformate decarboxylase in complex with a benzoylphosphonate inhibitor. *Biochemistry 48*, 3247–3257.
15. Bera, A. K., Polovnikova, L. S., Roestamadji, J., Widlanski, T. S., Kenyon, G. L., McLeish, M. J., and Hasson, M. S. (2007) Mechanism-based inactivation of benzoylformate decarboxylase, a thiamin diphosphate-dependent enzyme. *J. Am. Chem. Soc. 129*, 4120.
16. Bunik, V. I., Denton, T. T., Xu, H., Thompson, C. M., Cooper, A. J. L., and Gibson, G. E. (2005) Phosphonate analogues of α-ketoglutarate inhibit the activity of the α-ketoglutarate dehydrogenase complex isolated from brain and in cultured cells. *Biochemistry 44*, 10552–10561.
17. Frank, R. A. W., Price, A. J., Northrop, F. D., Perham, R. N., and Luisi, B. F. (2007) Crystal structure of the E1 component of the

Escherichia coli 2-oxoglutarate dehydrogenase multienzyme complex. *J. Mol. Biol. 368*, 639–651.
18. Wayne, L. G. (1994) Dormancy of *Mycobacterium tuberculosis* and latency of disease. *Eur. J. Clin. Microbiol. Infect. Dis. 13*, 908–914.
19. Weinstein, E. A., Yano, T., Li, L. S., Avarbock, D., Avarbock, A., Helm, D., McColm, A. A., Duncan, K., Lonsdale, J. T., and Rubin, H. (2005) Inhibitors of type II NADH:menaquinone oxidoreductase represent a class of antitubercular drugs. *Proc. Natl. Acad. Sci. U.S.A. 102*, 4548–4553.
20. Dhiman, R. K., Mahapatra, S., Slayden, R. A., Boyne, M. E., Lenaerts, A., Hinshaw, J. C., Angala, S. K., Chatterjee, D., Biswas, K., Narayanasamy, P., Kurosu, M., and Crick, D. C. (2009) Menaquinone synthesis is critical for maintaining mycobacterial viability during exponential growth and recovery from non-replicating persistence. *Mol. Microbiol. 72*, 85–97.
21. Truglio, J. J., Theis, K., Feng, Y. G., Gajda, R., Machutta, C., Tonge, P. J., and Kisker, C. (2003) Crystal structure of *Mycobacterium tuberculosis* MenB, a key enzyme in vitamin K-2 biosynthesis. *J. Biol. Chem. 278*, 42352–42360.
22. Lu, X. Q., Zhang, H. N., Tonge, P. J., and Tan, D. S. (2008) Mechanism-based inhibitors of MenE, an acyl-CoA synthetase involved in bacterial menaquinone biosynthesis. *Bioorg. Med. Chem. Lett. 18*, 5963–5966.
23. Sharma, S. K., Miller, M. J., and Payne, S. M. (1989) Spermexatin and spermexatol: New synthetic spermidine-based siderophore analogs. *J. Med. Chem. 32*, 357–367.
24. Riegel, B., and Lilienfeld, W. M. (1945) The synthesis of β-keto esters by the decomposition of acylated malonic esters. *J. Am. Chem. Soc. 67*, 1273–1275.
25. Rusnak, F., Liu, J., Quinn, N., Berchtold, G. A., and Walsh, C. T. (1990) Subcloning of the enterobactin biosynthetic gene EntB: Expression, purification, characterization, and substrate-specificity of isochorismatase. *Biochemistry 29*, 1425–1435.
26. Cornish-Bowden, A. (1995) Analysis of Enzyme Kinetic Data, Oxford University Press, New York.
27. Dixon, M. (1953) The determination of enzyme inhibitor constants. *Biochem. J. 55*, 170–171.
28. Cornish-Bowden, A. (1974) A simple graphical method for determining the inhibition constants of mixed, uncompetitive and noncompetitive inhibitors. *Biochem. J. 137*, 143–144.
29. Cho, S. H., Warit, S., Wan, B. J., Hwang, C. H., Pauli, G. F., and Franzblau, S. G. (2007) Low-oxygen-recovery assay for high-throughput screening of compounds against nonreplicating *Mycobacterium tuberculosis*. *Antimicrob. Agents Chemother. 51*, 1380–1385.
30. Franzblau, S. G., Witzig, R. S., McLaughlin, J. C., Torres, P., Madico, G., Hernandez, A., Degnan, M. T., Cook, M. B., Quenzer, V. K., Ferguson, R. M., and Gilman, R. H. (1998) Rapid, low-technology MIC determination with clinical *Mycobacterium tuberculosis* isolates by using the microplate Alamar Blue assay. *J. Clin. Microbiol. 36*, 362–366.
31. DeClue, M. S., Baldridge, K. K., Kast, P., and Hilvert, D. (2006) Experimental and computational investigation of the uncatalyzed rearrangement and elimination reactions of isochorismate. *J. Am. Chem. Soc. 128*, 2043–2051.
32. Karaman, R., Goldblum, A., Breuer, E., and Leader, H. (1989) Acylphosphonic acids and methyl hydrogen acylphosphonates: Physical and chemical properties and theoretical calculations. *J. Chem. Soc., Perkin Trans. 1*, 765–774.
33. Jarlier, V., and Nikaido, H. (1994) Mycobacterial cell wall: Structure and role in natural resistance to antibiotics. *FEMS Microbiol. Lett. 123*, 11–18.
34. Holm, L., and Park, J. (2000) DaliLite workbench for protein structure comparison. *Bioinformatics 16*, 566–567.
35. Lewendon, A., Murray, I. A., Shaw, W. V., Gibbs, M. R., and Leslie, A. G. W. (1990) Evidence for transition-state stabilization by serine-148 in the catalytic mechanism of chloramphenicol acetyltransferase. *Biochemistry 29*, 2075–2080.